This article has been accepted for publication in a future issue of this journal, but has not been fully edited. Content may change prior to final publication. Citation information: DOI 10.1109/TCOMM.2014.2385856, IEEE Transactions on Communications

Implementing the Han-Kobayashi Scheme Using Low Density Parity Check Codes over Gaussian Interference Channels

Shahrouz Sharifi, *Student Member*, *IEEE*, A. Korhan Tanc, *Member*, *IEEE*, and Tolga M. Duman, *Fellow*, *IEEE*

***Abstract*—We focus on Gaussian interference channels (GICs) and study the Han-Kobayashi (HK) coding strategy for the two-user case with the objective of designing implementable (explicit) channel codes. Specifically, low-density parity-check (LDPC) codes are adopted for use over the channel, their benefits are studied and suitable codes are designed. Iterative joint decoding is used at the receivers, where independent and identically distributed (i.i.d.) channel adapters are used to prove that log-likelihood-ratios (LLRs) exchanged among the nodes of the Tanner graph enjoy symmetry when BPSK or QPSK with Gray coding is employed. This property is exploited in the proposed code optimization algorithm adopting a *random perturbation technique*. Code optimization and convergence threshold computations are carried out for different GICs employing finite constellations by tracking the average mutual information. Furthermore, stability conditions for the *admissible* degree distributions under strong and weak interference levels are determined. Via examples, it is observed that the optimized codes using BPSK or QPSK with Gray coding operate close to the capacity boundary for strong interference. For the case of weak interference, it is shown that nontrivial rate pairs are achievable via the newly designed codes which are not possible by single user codes with time-sharing. Performance of the designed codes is also studied for finite block lengths through simulations of specific codes picked with the optimized degree distributions with random constructions, where, for one instance, the results are compared with those of some structured designs.**

***Index Terms*—Low-density parity-check codes, code design, Gaussian interference channels, Han-Kobayashi coding, iterative joint decoding.**

I. Introduction

There is a large body of work on two-user Gaussian interference channels (GICs), in which two independent transmitters communicate with their intended receivers through a shared medium. In spite of this intense research, full characterization of the capacity region is still an open problem, and only inner and outer bounds on achievable rates are available in the literature. The best reported inner bound to date is due to Han and Kobayashi referred as the Han-Kobayashi (HK) coding scheme [1]. Despite the superiority of the HK strategy, there is no work on exploring explicit and implementable channel codes adopting this technique in the current literature. With this motivation, in this paper, we study the design and performance of low-density parity-check (LDPC) codes over GICs implementing the HK strategy.

LDPC codes have been shown to achieve a performance extremely close to the Shannon limit for point-to-point (P2P) channels [2]. They have also been successfully applied to multi-user channels, where promising results have been obtained. For instance, capacity (or capacity bound) approaching codes are designed for two-user multiple-access channels (MACs), Gaussian broadcast channels, and relay channels [3]–[8]. There is also a recent work on the use of LDPC codes on symmetric GICs under weak interference [9]. However, there is no work in the existing literature on explicit code designs for GICs implementing the HK strategy in a practical manner.

In this paper, we investigate the performance of irregular LDPC codes over two-user GICs with fixed channel gains (also cf. [10]). We adopt finite constellations for transmission as Gaussian codebooks cannot be used due to practical transmission constraints such as synchronization, encoding, and decoding limitations. In the proposed scheme, the message of each transmitter is split into private and public parts encoded by separate LDPC codes. The encoded bits are modulated and superimposed to generate the transmitted signal. At each receiver, the public messages and the intended private message are jointly decoded in an iterative fashion.

Symmetry of the channel outputs considerably simplifies the analysis of the decoder for LDPC codes over P2P channels. In order to simplify the analysis for our multi-user setting in a similar manner, we exploit the independent and identically distributed (i.i.d.) channel adapters introduced in [11]. We propose a code optimization algorithm, based on a specific instance of differential evolution [12] where, at each iteration, perturbing vectors are utilized to generate the so-called *admissible* degree distributions for which the corresponding probability of decoding error tends to zero asymptotically. To simplify the design process, we prove a symmetry property of the exchanged log-likelihood-ratios (LLRs) within the joint decoder for BPSK and QPSK with Gray coding using the

S. Sharifi is with the School of Electrical, Computer and Energy Engineering (ECEE) of Arizona State University, Tempe, AZ 85287-5706, USA, (e-mail: sh.sharifi@asu.edu).

A. K. Tanc is with the Department of Electrical and Electronics Engineering, Kirklareli University, Kayali Campus, 39100, Kirklareli, Turkey (e-mail: korhan.tanc@kirklareli.edu.tr).

T. M. Duman is with the Department of Electrical and Electronics Engineering, Bilkent University, Bilkent, 06800, Ankara, Turkey, and is on leave from the School of ECEE of Arizona State University (e-mail: duman@ee.bilkent.edu.tr).

This work was presented in part at the 2014 IEEE International Symposium on Information Theory, Honolulu, Hawaii, July 2014.

Part of this publication, specifically Section 4, was made possible by NPRP grant 4-1293-5-213 from the Qatar National Research Fund (a member of Qatar Foundation). In addition, we also acknowledge support from National Science Foundation under the grant NSF-CCF 1117174 and from the European Commission under the grant MC-CIG PCIG12-GA-2012-334213 for Sections 1-3, 5-7. The statements made herein are solely the responsibility of the authors.

This article has been accepted for publication in a future issue of this journal, but has not been fully edited. Content may change prior to final publication. Citation information: DOI 10.1109/TCOMM.2014.2385856, IEEE Transactions on Communications

assumption that the Tanner graph of the joint decoder is cycle-free and the exchanged LLRs within the decoder are independent. The symmetry of the exchanged LLRs plays a key role in simplifying the mutual information calculations exploited to verify the admissibility of the perturbed degree distributions. Stability conditions are also derived for strong and weak interference levels employing BPSK and QPSK with Gray coding to ensure that the optimized codes do not suffer from elevated error floors.

Throughout the paper, for comparison purposes we will use naive and non-naive time sharing (TS) strategies. Under naive TS, we have individual power constraints for each user's transmitted symbols. This is motivated by the practical limitations in the transmission process, e.g., due to restrictions on the power amplifiers. Under non-naive TS the users can increase their individual power levels for a certain fraction of the total transmission time while keeping the average power over the entire codeword under a certain value.

Having implemented the HK strategy, we carry out the code optimization for symmetric and asymmetric GICs for various scenarios with different levels of interference. In all the investigated examples, it is observed that the optimized codes for the two-user GIC outperform P2P codes optimized for the binary-input additive white Gaussian noise (BI-AWGN) channel, and for most cases significant improvements are possible. Promising results are obtained under strong interference and rate pairs very close to the capacity boundaries are achieved. Under weak interference, the message of each transmitter is composed of private and public parts, therefore a power allocation optimization is performed prior to the code optimization. It is observed in this case that non-trivial rate pairs, which are not achievable with P2P codes used with TS, are attainable. We also provide simulation results with specific finite-length codes picked from the optimized code ensembles utilizing random constructions. Furthermore, the performance of the random constructions is compared to that of structured constructions utilizing an algebraic design approach.

The rest of the paper is organized as follows. In Section II, the system model is described, and computation of a sub-region of the HK achievable rate region (ARR) is summarized. In Section III, the implementation of the HK coding and decoding strategies and operations at the transmitter and receiver sides are described. In Section IV, i.i.d. channel adapters are introduced, a symmetry property of the exchanged LLRs under joint decoding is proved, stability conditions on the degree distributions of public and private messages are derived, and the proposed code optimization approach is detailed. In Section V, performance of the P2P and the optimized LDPC codes is investigated via a multitude of examples. In Section VI, finite block length code simulation results are provided, and finally, in Section VII, the paper is concluded.

II. System Model and Preliminaries

The input-output relationship for the two-user GIC (as illustrated in Fig. 1) is expressed as

$$\begin{aligned} Y_1 &= h_{11}X_1 + h_{21}X_2 + Z_1, \\ Y_2 &= h_{12}X_1 + h_{22}X_2 + Z_2, \end{aligned} \tag{1}$$

where h_{ij} is the fixed complex channel gain from the user i to the receiver j. Z_1 and Z_2 are i.i.d. circularly symmetric complex Gaussian noise samples with zero mean and $\frac{N_0}{2}$ variance per dimension. X_1 and X_2 are the transmitted complex signals with individual power constraints of P_1 and P_2, respectively, that is, $E\{|X_i|^2\} \leq P_i$ $(i = 1, 2)$. Signal-to-noise-ratio (SNR) and interference-to-noise-ratio (INR) at receiver i are defined as

$$SNR_i = \frac{|h_{ii}|^2 P_i}{N_0}, \quad INR_i = \frac{|h_{ji}|^2 P_j}{N_0},$$

where $i, j = 1, 2$ and $i \neq j$. Based on the interference and signal levels, the interference can be categorized as strong ($INR_i > SNR_j$), weak ($SNR_i > INR_j$), or mixed ($INR_i > SNR_j$, $INR_j < SNR_i$). For the case of a symmetric GIC, $h_{11} = h_{22}$, $h_{12} = h_{21}$, $SNR_1 = SNR_2 = SNR$, and $INR_1 = INR_2 = INR$.

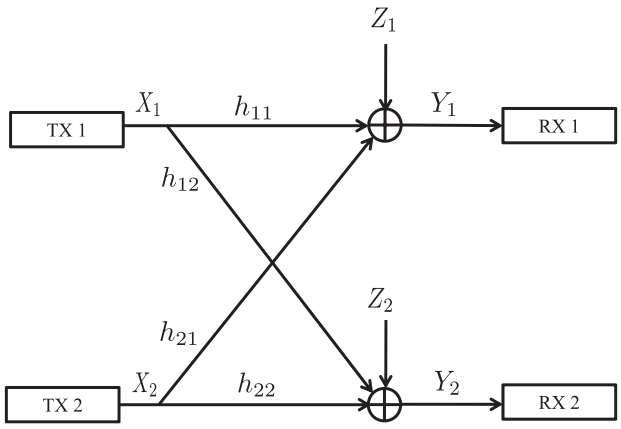

Fig. 1. Two-user GIC block diagram.

HK ARR Computation

The HK ARR is the best known inner bound on the capacity of interference channels. Under strong interference, this inner bound treats all messages as public [13] and characterizes the capacity region. Despite the superiority of the HK coding scheme, the computation of the entire rate region is prohibitively difficult since one should perform an optimization over the joint probability distribution of many random variables with large cardinalities. Authors in [14] provide a simplified expression of the rate region which is still difficult to compute. In this paper, the focus is on GICs, and instead of the entire region, a sub-region is obtained with a lower complexity by considering the superposition of independent uniformly distributed inputs from specific constellations as transmitted signals with no TS [1]. Denoting the code rates at the transmitters 1 and 2 by R_1 and R_2, respectively, the rate vector $\mathbf{R} = [R_1, R_2]^t$ is in the sub-region $\mathcal{R}_0$ if

$$\mathcal{R}_0 = \{\mathbf{R} | A\mathbf{R} \leq \Psi(P_1, P_2, \alpha_1, \alpha_2)\}, \tag{2}$$

where

$$\Psi = [\rho_1, \rho_2, \rho_{12}, \rho_{10}, \rho_{20}]^t,$$

$$A^t = \begin{bmatrix} 1 & 0 & 1 & 2 & 1 \\ 0 & 1 & 1 & 1 & 2 \end{bmatrix},$$

This article has been accepted for publication in a future issue of this journal, but has not been fully edited. Content may change prior to final publication. Citation information: DOI 10.1109/TCOMM.2014.2385856, IEEE Transactions on Communications

and α_i denotes the fraction of the power allocated to the private message of user i. In (2), the inequality sign is applied element-wise and Ψ is defined in [1, pp. 54–55]. As (2) suggests, different power allocations to the public and private messages give rise to different sub-regions. Thus, the above sub-region can be enlarged to

$$\mathcal{R}_1 = \bigcup_{(\alpha_1,\alpha_2)\in[0,1]\times[0,1]} \mathcal{R}_0(P_1, P_2, \alpha_1, \alpha_2).$$

Since $\mathcal{R}_1$ is not necessarily convex, it can be further enlarged by a convex hull operation. We denote the resulting sub-region by $\mathcal{R}$, which is an inner bound for the actual ARR. We note that, as mentioned in [1], the introduced inner bound may not cover the entire rate region obtained by non-naive TS. For instance, Fig. 9 demonstrates the inner bounds (HK ARR) $\mathcal{R}_1$ for a finite constellation and for Gaussian signaling where it is clear that the non-naive TS rate region is not contained within the inner bound $\mathcal{R}_1$.

There are four main outer bounds for the rate region of GICs in the literature. The first bound is obtained in [15] for the degraded GIC based on the capacity region of a specific degraded broadcast channel. The second is due to Kramer for a GIC with weak interference where the bound is attained by discarding one of the interfering links in the channel [16]. The third is proposed by Etkin *et al.* for a general GIC exploiting a genie-aided technique [17]. The fourth, which is the most recent one, is reported by Motahari and Khandani based on the concept of *admissible channels* [18]. In this paper, we use the results of [17] since the bounds require only simple calculations and are shown to be within one bit of the capacity region.

III. Implementation of the HK Encoding and Decoding Scheme

A. Encoding

Considering the HK coding scheme, the message of each user is divided into two parts, namely, the private message (U) and the public message (W). The public messages are decodable at both receivers while the private messages are only decodable at the intended receivers. Although in the general scheme messages are split into public and private parts, there are special cases where there may be no need to allocate the power to both; for instance, under strong interference, both users' messages are public (and no private message is transmitted) since all the messages are decodable at both receivers.

Fig. 2 shows the block diagram of the transmitter incorporating the HK coding scheme wherein the messages of each transmitter (U and W) are encoded with separate LDPC codes (resulting in C_u and C_w). The resulting bits are then modulated (denoted by X_u and X_w) and superimposed to form the overall transmitted signal (X). Here, we superimpose the two signals with standard addition; however, it is also possible to consider other alternatives. For instance, superimposing of two signals can be done in the "code" domain through modulo-2 addition (which may be the proper choice in the case of binary input channels), however, this scheme would require a different code optimization which is out of the scope of this paper. As another example, it is also possible to consider higher order signal constellations, and perform mappings of the public and private coded bits to the constellation points jointly. It should further be emphasized that our focus is on practical modulation techniques such as PSK signaling since Gaussian signaling (as usually assumed in information theoretic studies) cannot be used in practical systems.

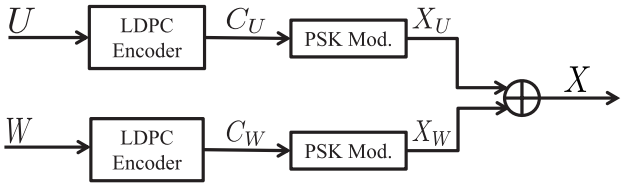

Fig. 2. Construction of the transmitted signal for the proposed implementation of the HK coding scheme.

B. Decoding

At the receiver side, the public messages and the private message of the desired user are decoded by utilizing a belief-propagation (BP) algorithm wherein the soft-information about the messages are exchanged within the decoder in an iterative fashion [19]. Different decoding schemes are possible, namely, successive interference cancellation (SIC) (see, e.g. [20], [21]) and joint decoding (JD) [3], as illustrated in Figs. 3(a) and 3(b).

In SIC, decoding is done sequentially adopting component LDPC decoders where the decoded messages at each stage are subtracted from the original signal until all the messages are estimated. It is possible to improve the overall performance by iterating between the component LDPC decoders. Under JD, in contrast to SIC, decoding of the messages are performed concurrently and in rounds. Each round starts with computing the LLRs to be fed to the component LDPC decoders, where each decoder runs for some iterations utilizing the BP algorithm. The round is completed by passing the updated LLRs from the variable nodes to the so-called state nodes, denoted with the black circle in the figure. In the following, we discuss the details of the joint decoding employed throughout the paper.

1) Scheduling: The exchange of LLRs between the component LDPC decoders and the state nodes can be performed serially or in parallel. In parallel scheduling all component LDPC decoders run simultaneously whereas in serial scheduling only one component LDPC decoder is active at each iteration [3]. This process is repeated until all the messages are decoded, or a predetermined number of iterations is reached.

2) LLR Computation at the State Nodes: The LLR of the ith coded bit of message j at receiver k is computed as

$$L\big(c_j(i), Y_k(i)\big) = \log\left(\frac{f_{Y_k}\big(Y_k(i)|c_j(i)=0\big)}{f_{Y_k}\big(Y_k(i)|c_j(i)=1\big)}\right), \qquad (3)$$

where $c_j(i)$ is the ith coded bit of message j, which can be a public message or the intended private message, and f_{Y_k} represents the probability density function (PDF) of Y_k. Considering parallel scheduling, upon the start of each iteration,

This article has been accepted for publication in a future issue of this journal, but has not been fully edited. Content may change prior to final publication. Citation information: DOI 10.1109/TCOMM.2014.2385856, IEEE Transactions on Communications

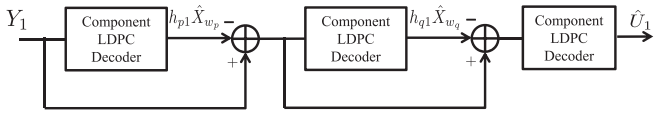

(a) SIC block diagram

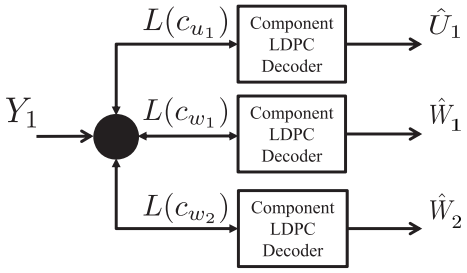

(b) Joint decoder block diagram.

Fig. 3. Block diagram of the decoder structures at receiver 1 ($p, q = 1, 2,\ p \neq q$). $\hat{X}$ denotes the decoded message for the transmitted message X.

the LLR corresponding to $c_j(i)$ provided to the component LDPC decoder of message j is computed at the state nodes by marginalization, that is,

$$L\big(c_j(i), Y_k(i)\big) = \log\left(\frac{\sum_{C_i \in S_i^{j+}} f_{Y_k}\big(Y_k(i)|C_i\big)P\big(C_i\big)}{\sum_{C_i \in S_i^{j-}} f_{Y_k}\big(Y_k(i)|C_i\big)P\big(C_i\big)}\right), \tag{4}$$

where C_i is the vector comprising the ith coded bits of all public and private codewords, i.e., $C_i = \{c_{u_1}(i), c_{w_1}(i), c_{u_2}(i), c_{w_2}(i)\}$ and $P(C_i)$ denotes the probability of C_i which is determined by the outputs of component LDPC decoders and gets updated at each iteration. S_i^{j+} and S_i^{j-} denote the subsets of the codewords with $c_j(i) = 0$ and $c_j(i) = 1$, respectively. Note that at the receiver r, U_k ($k \neq r$) is not decoded, hence, the corresponding component in C_i does not get updated and remains constant throughout the iterations. The computation of the extrinsic LLRs at the state nodes for BPSK differs from that for higher order modulations such as QPSK. For BPSK, the extrinsic LLRs sent to each component LDPC decoder are updated based on the received LLRs from other component LDPC decoders. In contrast, for higher order modulations, the LLR sent from each variable node to the connected state node contributes to the updated extrinsic LLR sent to its neighbor node(s) from that state node. For instance, Fig. 4 illustrates a portion of the joint decoder for QPSK, where each state node is connected to two variable nodes, hence, the LLR sent from each variable node to the state node contributes to the updated extrinsic LLR sent to its neighbor.

IV. Analytic Properties and Optimization of LDPC Codes over GICs

The objective in this section is to develop an optimization method for LDPC code ensembles over GICs. Irregular LDPC codes have previously been employed for communication over

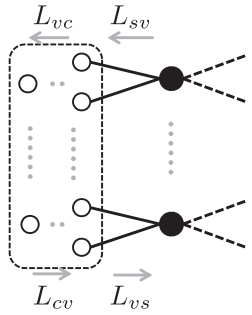

Fig. 4. The Tanner graph representation of LDPC codes with QPSK mapping. L_{cv}, L_{vc}, L_{sv}, and L_{vs} represent the extrinsic LLRs sent from the check nodes to the variable nodes, variable nodes to the check nodes, state nodes to the variable nodes, and variable nodes to the state nodes, respectively.

different multi-user channels due to their excellent performance [3], [5], [6]. In this paper, we follow similar ideas, and consider their use over GICs. Following the notation in [2], an ensemble of irregular LDPC codes (λ, ρ) is described with

$$\lambda(x) = \sum_{i=2}^{d_v} \lambda_i x^{i-1} \quad \text{and} \quad \rho(x) = \sum_{i=2}^{d_c} \rho_i x^{i-1},$$

where d_v and d_c are the maximum degrees of variable and check nodes, respectively, and the *design rate* of the LDPC code is

$$r = 1 - \frac{\sum_i \rho_i / i}{\sum_i \lambda_i / i}.$$

An LDPC code ensemble is shown to exhibit arbitrarily small error probability under iterative decoding beyond a certain threshold. The threshold for P2P AWGN channels is controlled by the noise power, however, for GICs, the channel gains for the direct and the interference links are also required for its characterization.

Density evolution is the most accurate available tool to calculate the threshold of an LDPC code ensemble. This method tracks the PDF of the exchanged LLRs between the variable and check nodes analytically; however, under joint decoding, due to the non-linearity of the update rule at the state nodes, it is very difficult to characterize the PDF of the outgoing LLRs from the state nodes. Furthermore, the computation becomes cumbersome for multiuser scenarios where the PDFs of multiple users' LLRs are involved. An EXIT chart analysis is an alternate method which tracks the mutual information evolution between the transmitted bits and exchanged LLRs wherein the PDF of the LLRs are assumed to be Gaussian. Although the Gaussianity assumption simplifies the code design procedure and has lead to well-performing codes for certain multi-user channels, our implementations show that this approximation leads to imprecise results when a joint decoder is employed as in our set-up. In other words, for certain ranges of the channel parameters, the thresholds obtained with Gaussian assumption significantly differ from the ones obtained through finite block length code simulations. Therefore, we propose a code optimization utilizing a specific instance of differential evolution algorithm wherein the convergence of the joint decoder for the adopted degree

This article has been accepted for publication in a future issue of this journal, but has not been fully edited. Content may change prior to final publication. Citation information: DOI 10.1109/TCOMM.2014.2385856, IEEE Transactions on Communications

distributions is checked by tracking the evolution of the mutual information with no Gaussianity assumption on the exchanged LLRs.

In the following, we review i.i.d. channel adapters and prove a symmetry property of the exchanged LLRs within the joint decoder. Furthermore, we study the stability conditions for the degree distributions of the public and private messages for different interference levels.

A. I.I.D. Channel Adapters

Symmetry of the channel output is defined as

$$f_Y(Y(i)|c(i)=0) = f_Y(-Y(i)|c(i)=1),$$

where $Y(i)$ and $c(i)$ refer to the ith channel output and the ith coded bit, respectively. This property greatly simplifies the decoding analysis of LDPC codes [22]. Unfortunately, the property does not hold for multi-user scenarios. To remedy this problem, the authors in [11] introduced a tool called i.i.d. channel adapters enforcing the symmetry of the channel outputs for multi-user channels wherein random sequences are deployed with common randomness at the transmitter and receiver sides for each message. We note that an alternative is to use the chaining technique described in [23], which does not require sharing of common randomness between each pair of the transmitters and the receivers. Here, we utilize the i.i.d. channel adapters for private and public messages to make sure that the channel outputs are symmetric and analysis becomes tractable; however, it should be noted that the i.i.d. channel adapters are employed to simplify the analysis and are not implemented during the actual encoding and decoding processes.

B. LLR Symmetry Property

The PDF of the LLRs sent from the state nodes to the component LDPC decoder of message j is symmetric if

$$l = \log\Big(\frac{f_L(l|c_j(i)=0)}{f_L(-l|c_j(i)=0)}\Big), \qquad l \in \mathbb{R}.$$

It is shown in [24] that for a BI-AWGN channel the symmetry property holds for the PDF of the channel LLRs delivered to the iterative decoder and the property is preserved for the exchanged LLRs in the decoder throughout the decoding iterations. In contrast to BI-AWGN channels, for multi-user channels, wherein a joint decoder is employed at the receiver, the LLRs sent from the state nodes to each component LDPC decoder depend on both the channel LLRs and the extrinsic LLRs received from the other component LDPC decoders. In the following, we prove the symmetry property for the LLRs exchanged within the joint decoder for the considered GICs adopting BPSK or QPSK with Gray coding.

Theorem 1. *Consider a receiver in a two-user output-symmetric GIC for which the private and public messages are obtained by BPSK or QPSK with Gray coding*[1]*. For a joint decoder with a cycle free Tanner graph, the extrinsic LLR sent from the state node to the variable node of the component LDPC decoder of message j is inverted if the signs of the channel outputs and the a-priori LLRs received from the other component LDPC decoders are inverted.*

Proof: We denote the LLR sent from the state node to the variable node of the component LDPC decoder of message j obtained by inverting the signs of the channel outputs and the a-priori LLRs received from the other component LDPC decoders by L'_{sv} and show that

$$L_{sv} = -L'_{sv}. \tag{5}$$

We show the property for QPSK with Gray coding, and simply note that the case of BPSK can be handled similarly. Considering Gray coding, the real and imaginary parts of the ith transmitted symbol $X_m(i)$ (m can be a public message or the intended private message) are $\sqrt{\frac{P_m}{2}}(1-2c_m(2i))$ and $\sqrt{\frac{P_m}{2}}(1-2c_m(2i+1))$, respectively. It can easily be shown that

$$\begin{aligned} P\big(Re(X_m(i)) = \pm\sqrt{\tfrac{P_m}{2}}\big) &= \frac{\exp\big(\pm L_{vs}(c_m(2i))\big)}{1+\exp\big(\pm L_{vs}(c_m(2i))\big)}, \\ P\big(Im(X_m(i)) = \pm\sqrt{\tfrac{P_m}{2}}\big) &= \frac{\exp\big(\pm L_{vs}(c_m(2i+1))\big)}{1+\exp\big(\pm L_{vs}(c_m(2i+1))\big)}. \end{aligned} \tag{6}$$

Using (4), (6), and the fact that LLRs sent along all the edges in a cycle free Tanner graph are independent, (5) follows completing the proof. ■

Considering (3) and Theorem 1, it is easy to show that the symmetry property of the LLRs sent from the state nodes to the variable nodes holds, and since the property is preserved under BP [2], the property holds for all the LLRs exchanged within the joint decoder. The symmetry property of the LLRs can be exploited to show that [25]

$$I(L;c) = 1 - E\big\{\log_2(1+e^{-L})\big\}, \tag{7}$$

where $I(L;c)$ denotes the mutual information between the exchanged LLR L and the corresponding coded bit c assuming that the all zero-codeword is transmitted. The expectation in (7) can be computed by invoking the ergodicity assumption for the exchanged LLRs. As a result, the mutual information calculations can be performed without requiring the analytical PDFs of the exchanged LLRs, which plays a key role in the proposed code optimization approach.

C. Stability Condition

The stability condition was first introduced in [2] to analyze the convergence behavior of the iterative decoder when the probability of the decoding error is close to zero. It was also examined in the context of Gaussian broadcast channels in [5] for a cycle free joint decoder with two component decoders. Here, we analyze the stability conditions for the joint decoder adopted for the two-user GIC when the HK strategy is implemented for different cases. For the sake of analysis, we assume that the joint decoder has run for a sufficient number of iterations so that the performance of each component LDPC

[1]The result also holds for higher order modulations if the corresponding constellation is symmetric with respect to origin and the sequences of bits assigned to two symmetric points in the constellation are flipped versions of one another.

This article has been accepted for publication in a future issue of this journal, but has not been fully edited. Content may change prior to final publication. Citation information: DOI 10.1109/TCOMM.2014.2385856, IEEE Transactions on Communications

decoder has reached to steady state. To analyze the stability condition, similar to [5], the PDFs of the LLRs corresponding to the ith coded bit of message m (m can be a public message or the intended private message), sent from the check nodes to the ith variable node of the corresponding component LDPC decoder, conditioned on having transmitted all-zero codeword for message m, is expressed as

$$f_L(l) = (1-\epsilon_m)\Delta_\infty + \epsilon_m \Delta_0, \tag{8}$$

where Δ_a denotes the Dirac delta function at a and $\epsilon_m \approx 0$ is the probability of the error for message m. Note that the assumption of transmitting the all-zero codeword is valid for all the messages when channel adapters are employed. For a cycle free Tanner graph, the PDF of the LLRs sent from the variable nodes to the state nodes evolves from (8) to

$$f_L(l) = (1-\epsilon_m^2)\Delta_\infty + \mathcal{O}(\epsilon_m^2), \tag{9}$$

which implies that $P\big(c_m(i)=0\big) = 1-\epsilon_m^2$. Considering (4), at the receiver k, the update rule at the state nodes for $L\big(c_j(i), Y_k(i)\big)$, can be written as

$$L\big(c_j(i), Y_k(i)\big) = L\big(c_j(i), Y_k'(i)\big) + \mathcal{O}(\epsilon^2),$$

where j can be a public message or the intended private message and $\epsilon = \max\{\epsilon_{m_1}, \epsilon_{m_2}\}$. $Y_k'(i)$ is the ith modified channel output symbol with respect to the message j at the receiver k, which is obtained by removing the effect of the messages m_1 and m_2. To simplify the analysis, we neglect the effect of $\mathcal{O}(\epsilon^2)$ and work with the modified channel output Y_k'.

Following the approach taken in [5], we derive the stability conditions for the degree distributions of public and private messages under strong and weak interference levels. Note that both receivers should be analyzed in deriving the stability condition for the degree distributions of public messages while for the degree distribution of each private message only the intended receiver needs to be considered. Since the computations of the LLRs at the state nodes for real and complex signaling are not the same (refer to Fig. 3 and Fig. 4), we separately derive the conditions for BPSK with real channel gains and QPSK with Gray coding with complex channel gains.

1) Strong Interference: Under strong interference the messages are transmitted as public, therefore the stability condition is only derived for the degree distributions of public messages. *BPSK with Real Channel Gains*: For this case, the channel gains and the transmitted symbols are real, hence the imaginary part of the received signal can be discarded. At receiver k, the modified channel output with respect to W_i is obtained as

$$Y_k' = h_{ik} X_{w_i} + \mathrm{Re}(Z_k),$$

which resembles a P2P channel and the existing results in [2] can be utilized. Considering both receivers, since $INR_j > SNR_i \ , i \neq j$, the stability condition for $(\lambda_{w_i}, \rho_{w_i})$ is expressed as

$$\lambda_{w_i}'(0)\rho_{w_i}'(1) < e^{SNR_i}, \quad i = 1, 2.$$

QPSK with Gray Coding and Complex Channel Gains: For QPSK with Gray coding, each state node in the Tanner graph of the joint decoder is connected to two successive variable nodes corresponding to the real part and the imaginary part of the transmitted symbol. Without loss of generality, we consider the variable node corresponding to the real part of the transmitted symbol X_{w_i} in the joint decoder at the receiver k. The modified channel output with respect to $\mathrm{Re}(X_{w_i})$ is obtained as

$$Y_k' = h_{ik}\,\mathrm{Re}(X_{w_i}) + Z_k.$$

Therefore, similar to the previous case, the stability condition for $(\lambda_{w_i}, \rho_{w_i})$ is

$$\lambda_{w_i}'(0)\rho_{w_i}'(1) < e^{\frac{SNR_i}{2}}, \quad i = 1, 2.$$

2) Weak Interference: Under weak interference, the two public messages and the intended private message are decoded at each receiver, i.e., the private message of the interfering signal is not decoded, and the corresponding part is present in the modified channel output.

BPSK with Real Channel Gains: For this scenario, the modified channel output at the receiver k with respect to the message U_k is

$$Y_k' = h_{kk}X_{u_k} + h_{rk}X_{u_r} + \mathrm{Re}(Z_k) \quad k \neq r,$$

which is similar to the channel studied in [5], hence the stability condition for $(\lambda_{u_k}, \rho_{u_k})$ is given by

$$\lambda_{u_k}'(0)\rho_{u_k}'(1) < \Bigg(e^{-\alpha_k SNR_k - \alpha_r INR_k} \times E_{N_1}\Bigg\{ \sqrt{\tfrac{\cosh(2N_1\sqrt{2\alpha_r INR_k}) + \cosh(4\sqrt{\alpha_r\alpha_k SNR_k INR_k})}{2}} \Bigg\} \Bigg)^{-1},$$

where E_{N_1} denotes the expectation taken with respect to a standard Gaussian random variable $N_1 \sim \mathcal{N}(0,1)$. Similarly, the modified channel outputs with respect to W_k at the receiver k and r ($k \neq r$) are obtained as

$$Y_k' = h_{kk}X_{w_k} + h_{rk}X_{u_r} + \mathrm{Re}(Z_k),$$
$$Y_r' = h_{kr}(X_{w_k} + X_{u_k}) + \mathrm{Re}(Z_r).$$

Considering both receivers, the stability condition for $(\lambda_{w_k}, \rho_{w_k})$ is obtained as

$$\lambda_{w_k}'(0)\rho_{w_k}'(1) < \min\Bigg\{ \Bigg(e^{-(1-\alpha_k)SNR_k - \alpha_r INR_k} \times E_{N_1}\Bigg\{ \sqrt{\tfrac{\cosh(2N_1\sqrt{2\alpha_r INR_k}) + \cosh(4\sqrt{(1-\alpha_k)\alpha_r SNR_k INR_k})}{2}} \Bigg\} \Bigg)^{-1}, \Bigg(e^{-INR_r} \times E_{N_1}\Bigg\{ \sqrt{\tfrac{\cosh(2N_1\sqrt{2\alpha_k INR_r}) + \cosh(4INR_r\sqrt{(1-\alpha_k)(\alpha_k)})}{2}} \Bigg\} \Bigg)^{-1} \Bigg\}.$$

QPSK with Gray Coding and Complex Channel Gains: Similar to the strong interference case, we consider the LLR sent from the state node to the variable node corresponding to the real part of the message of interest. Therefore, the modified channel

This article has been accepted for publication in a future issue of this journal, but has not been fully edited. Content may change prior to final publication. Citation information: DOI 10.1109/TCOMM.2014.2385856, IEEE Transactions on Communications

output with respect to U_k is obtained as

$$Y_k' = h_{kk}\,\mathrm{Re}(X_{u_k}) + h_{rk}X_{u_r} + Z_k,$$

where $k \neq r$. The stability condition for $(\lambda_{u_k}, \rho_{u_k})$ can be obtained by computing the Bhattacharyya constant [5] for the modified channel output resulting in

$$\lambda'_{u_k}(0)\rho'_{u_k}(1) < \left(e^{-\frac{\alpha_k SNR_k}{2} - \alpha_r INR_k} \times E_{N_1N_2}\left\{\sqrt{g(N_1, N_2, h_{kk}\sqrt{\tfrac{\alpha_k P_k}{2}}, h_{rk}\sqrt{\tfrac{\alpha_r P_r}{2}})}\right\}\right)^{-1},\ r \neq k,$$

where N_1 and N_2 are Gaussian random variables with zero mean and variance $\frac{1}{2}$, and

$$\begin{aligned} &g(N_1, N_2, A_1, A_2) \\ &= \tfrac{1}{16}\sum_{a=0}^{1}\sum_{b=0}^{1}\sum_{c=0}^{1}\sum_{d=0}^{1}\exp\Bigg(\tfrac{1}{N_0}\Big(2N_1\Big(A_{2_i}(-1)^a - A_{2_q}(-1)^b + A_{2_i}(-1)^c - A_{2_q}(-1)^d\Big) - 2A_{1_i}\Big(A_{2_i}(-1)^a \\ &\quad - A_{2_q}(-1)^b - A_{2_i}(-1)^c + A_{2_q}(-1)^d\Big) + 2N_2\Big(A_{2_i}(-1)^b + A_{2_q}(-1)^a + A_{2_i}(-1)^d + A_{2_q}(-1)^c\Big) - 2A_{1_q}\Big(A_{2_i}(-1)^b \\ &\quad + A_{2_q}(-1)^a - A_{2_i}(-1)^d - A_{2_q}(-1)^c\Big)\Big)\Bigg), \end{aligned} \tag{10}$$

where A_{j_i} and A_{j_q} in (10) denote the real and imaginary parts of A_j, respectively, with $j = 1, 2$. Similar analysis can be performed for $(\lambda_{w_k}, \rho_{w_k})$ considering both receivers, where the stability condition is expressed as

$$\lambda'_{w_k}(0)\rho'_{w_k}(1) < \min\left\{\left(e^{-\frac{(1-\alpha_k)SNR_k}{2} - \alpha_r INR_k} \times E_{N_1N_2}\left\{\sqrt{g(N_1, N_2, h_{kk}\sqrt{\tfrac{(1-\alpha_k)P_k}{2}}, h_{rk}\sqrt{\tfrac{\alpha_r P_r}{2}})}\right\}\right)^{-1}, \left(e^{-\frac{(1+\alpha_k)INR_r}{2}} \times E_{N_1N_2}\left\{\sqrt{g(N_1, N_2, h_{kr}\sqrt{\tfrac{(1-\alpha_r)P_r}{2}}, h_{kr}\sqrt{\tfrac{\alpha_r P_r}{2}})}\right\}\right)^{-1}\right\}.$$

D. Proposed Code Optimization Method

To initialize the code optimization procedure, for each of the involved messages, we select the degree distributions of the LDPC codes among the optimized P2P codes for BI-AWGN channels (obtained via the EXIT chart method in [26]). The selected degree distributions are then employed for the two-user GIC and checked whether they are admissible for the given channel parameters, that is, if the probability of decoding error for the corresponding code goes to zero asymptotically. To verify this, we assume that the joint decoder is cycle free and run the decoder with a sufficient number of state nodes (taken as 10^6 in our examples) fed with realizations of the channel outputs. The employed degree distributions are declared admissible if, for each component LDPC decoder, the mutual information between the transmitted bits and the exchanged LLRs within the component LDPC decoder evolves to 0.995. Note that we do not simulate any specific code realization, hence the adopted method captures the average behavior of the code ensembles by tracking the evolution of the mutual information without using any Gaussianity assumption for the PDFs of the exchanged LLRs within the joint decoder.

Having obtained the admissible degree distributions, perturbing vectors are utilized to generate a new instance of degree distributions with increased rates following the approach utilized in [27] in an iterative fashion. To simplify the code optimization, we assume that the check node degree distribution is a singleton and it does not change throughout the iterations; therefore, only the variable node degree distribution is perturbed as $\tilde{\lambda}_i = \lambda_i + e_i$, where e_i denotes the ith element of the perturbing vector and $\tilde{\lambda}_i$ represents the ith coefficient of $\tilde{\lambda}$. For the variable node degree distribution to be valid, $\sum_{i=2}^{d_v}\tilde{\lambda}_i = 1$, which enforces

$$\sum_{i=2}^{d_v} e_i = 0 \quad \text{and} \quad 0 \leq \lambda_i + e_i \leq 1. \tag{11}$$

At each iteration, the current rate (r_0) is increased by the rate increment K, that is,

$$1 - \frac{1}{d_c}\frac{1}{\sum_i \frac{\tilde{\lambda}_i}{i}} = r_0 + K,$$

which implies that

$$\sum_i \frac{\tilde{\lambda}_i}{i} = \frac{1}{d_c\big(1 - r_0 - K\big)},$$

resulting in

$$\sum_i \frac{e_i}{i} = \frac{K}{d_c\big((1-r_0)^2 - K(1-r_0)\big)}. \tag{12}$$

The perturbing vector is generated by drawing all the elements except two from a standard normal distribution, i.e., $\mathcal{N}(0, 1)$. The remaining two elements are obtained by solving the set of linear equations (11) and (12). The perturbing vector is adopted if it meets the inequality constraints in (11) and the resulting degree distributions satisfy the stability condition, otherwise a new perturbing vector is generated. The perturbed variable node degree distribution replaces the current one if the resulting degree distributions are admissible, otherwise it is dismissed and a new perturbation is performed. The process is stopped if no new admissible degree distributions can be found after a predetermined number of perturbations.

Remark: Although we have assumed a singleton distribution for the check nodes, this constraint can be relaxed by adding a separate perturbing vector. In this case, both the check node and the variable node degree distributions are perturbed jointly where the constraints on the perturbing vectors should be changed accordingly. Note that the proposed optimization is not limited to a specific modulation, however, in order to exploit the symmetry property of the LLRs in the computation of (7), the employed constellation should be symmetric with respect to origin and the sequences of bits assigned to two symmetric points in the constellation should be flipped versions of one another.

This article has been accepted for publication in a future issue of this journal, but has not been fully edited. Content may change prior to final publication. Citation information: DOI 10.1109/TCOMM.2014.2385856, IEEE Transactions on Communications

V. Examples of LDPC Codes Over GICs

In this section, we investigate the performance of irregular LDPC codes adopted for transmission over two-user GICs implementing the HK coding/decoding strategy. We restrict our attention to the case of fixed channel gains and finite signal constellations. A range of examples for different interference levels employing BPSK and QPSK with Gray coding are studied. In all the instances, code optimization is performed for symmetric and asymmetric rate pairs with the goal of sum rate maximization where the rate increments are along a straight line in the rate region. We select a variable node degree distribution with a maximum degree of 50. Motivated by [2], nonzero variable node degrees are selected as $\{2, 3, 4, 9, 10, 19, 20, 49, 50\}$, although there is no guarantee that this is the best choice. For the check nodes, we opt for a singleton distribution, i.e., $\rho(x) = x^{d_c-1}$, which is kept fixed throughout the code optimization process. The degree of the check nodes (d_c) is determined by optimizing the initial degree distribution for a BI-AWGN channel utilizing the EXIT chart analysis [26]. The performance of the optimized codes for the two-user GIC is compared with that of the P2P codes optimized for a BI-AWGN achieving the highest sum-rate, which does not necessarily correspond to the initial degree distributions. The degree distributions of the optimized codes and the P2P codes are presented in the Appendix. Note that for symmetric channels, the degree distributions corresponding to the rate pair (R_1, R_2) can also be used to achieve (R_2, R_1) by interchanging the employed degree distributions. Moreover, for symmetric rate pairs (i.e., when $R_1 = R_2$) achieved for symmetric channels, identical degree distributions (with distinct code realizations) are adopted for the messages of both users.

A. GIC with Strong Interference

Under strong interference, all the messages are public and the capacity region is known. Although the capacity region is determined by those of two MACs, the code design method in [3] is not directly applicable since the channel gains are not equal in general, and each message should be decodable at each of the receivers. In the following, we study several different scenarios.

Scenario I – Symmetric GIC with BPSK: For this instance, a symmetric GIC is considered, whose capacity regions with different inputs and achieved rate pairs are shown in Fig. 5. The best achievable rate pairs obtained with P2P codes are also depicted in Fig. 5. It can be observed that, for the optimized codes, the achieved rate pairs are close to the boundary of the capacity region and they outperform the P2P codes. Moreover, the P2P codes and the optimized codes perform better than the single user codes with non-naive TS.

Scenario II – Asymmetric GIC with BPSK: In this example, an asymmetric GIC with channel parameters shown in Fig. 6 is considered. Unlike the previous example, for both symmetric and asymmetric rate pairs, two degree distributions are optimized separately since the channels observed by each receiver are different. It can be observed that, similar to the previous example, the achieved rate pairs for the optimized degree distributions outperform the ones obtained with the P2P codes. Furthermore, all the achieved rate pairs with the P2P and optimized codes are superior to the ones obtained via the single user codes utilizing non-naive TS.

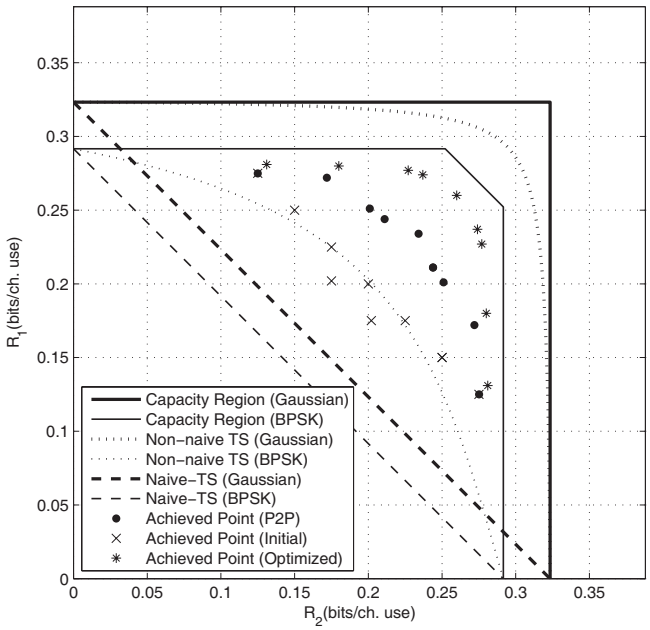

Fig. 5. Scenario I: capacity regions and achieved rate pairs for a symmetric GIC with strong interference. $SNR = -6$ dB, $INR = -5$ dB.

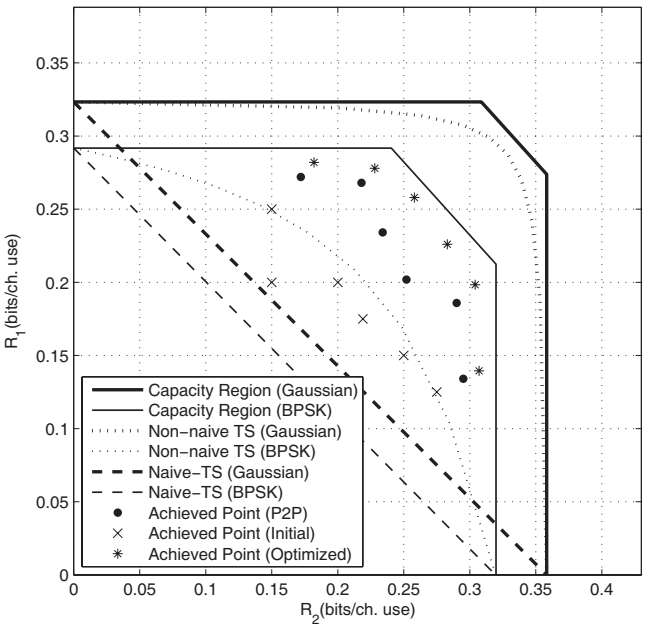

Fig. 6. Scenario II: capacity regions and achieved rate pairs for an asymmetric GIC with strong interference. $SNR_1 = -6$ dB, $INR_1 = -5.25$ dB, $SNR_2 = -5.5$ dB, $INR_2 = -4.75$ dB.

Scenario III – Symmetric GIC with QPSK: The details for this example are given in Fig. 7. The code optimization is performed for both symmetric and asymmetric rate pairs. Similar to the BPSK example, only one code is optimized for both messages when symmetric rate pairs are considered.

This article has been accepted for publication in a future issue of this journal, but has not been fully edited. Content may change prior to final publication. Citation information: DOI 10.1109/TCOMM.2014.2385856, IEEE Transactions on Communications

We observe that the achieved rate pairs with optimized codes outperform the ones obtained with P2P codes, and that both optimized and P2P codes beat the non-naive TS results with QPSK inputs. Furthermore, the optimized codes even outperform the non-naive TS results with Gaussian signaling.

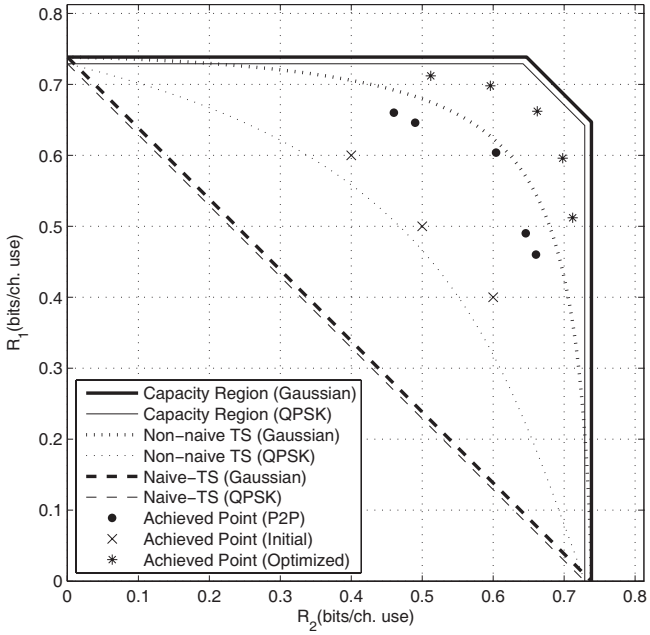

Fig. 7. Scenario III: capacity regions and achieved rate pairs for a symmetric GIC with strong interference. $SNR = -1.75$ dB, $INR = -0.25$ dB, $\angle\, h_{11} = \angle\, h_{22} = \frac{\pi}{4}$, $\angle h_{21} = \angle h_{12} = \frac{\pi}{3}$.

Scenario IV – Asymmetric GIC with QPSK: For this example, an asymmetric channel is considered, and the corresponding results are depicted in Fig. 8. Degree distributions are optimized for both symmetric and asymmetric rate pairs. Parallel to our previous findings, the optimized codes perform better than the P2P codes both of which operating outside the non-naive TS rate region. Specifically, all of the optimized codes and one instance of the P2P codes outperform the single user codes with Gaussian signaling with non-naive TS.

B. GIC with Weak Interference

Under weak interference, the interfering signal cannot be decoded in its entirety, and hence sending all the messages as public may not be optimal. As a result, unlike the case of strong interference, power allocation should be addressed prior to the code optimization. To simplify the process, an optimization problem is solved to achieve the largest rate region formulated as

$$\begin{aligned} \max_{\alpha_1,\alpha_2} \quad & R_{u_1} + R_{w_1} + R_{u_2} + R_{w_2} \\ \text{subject to} \quad & \Big\{R_{u_1}(\alpha_1), R_{w_1}(\alpha_1), R_{u_2}(\alpha_2), R_{w_2}(\alpha_2)\Big\} \in \mathcal{R}_1 \\ & 0 \le \alpha_i \le 1, \quad i = 1, 2, \\ & R_{u_1} + R_{w_1} = R_{u_2} + R_{w_2} + \Delta R, \end{aligned} \tag{13}$$

where R_{u_i} and R_{w_i} denote the rates of the messages U_i and W_i at the transmitter i, respectively. All the rates in (13) should be contained in the HK sub-region $\mathcal{R}_1$ characterized through (2) computed for the employed constellations (BPSK or QPSK with Gray coding), for which no time sharing is utilized and the private message and the public message of each transmitter is combined through addition. The last constraint in (13) is added to simplify the optimization process where ΔR is an arbitrary value also employed and kept fixed during the code optimization.

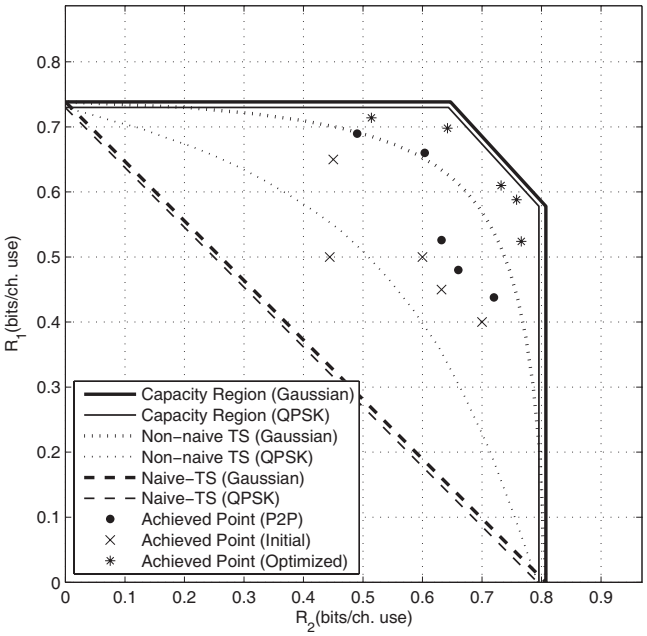

Fig. 8. Scenario IV: capacity regions and achieved rate pairs for an asymmetric GIC with strong interference. $SNR_1 = -1.75$ dB, $INR_1 = -0.25$ dB, $SNR_2 = -1.25$ dB, $INR_2 = 0.25$ dB, $\angle h_{11} = \frac{\pi}{4}$, $\angle h_{21} = \frac{\pi}{3}$, $\angle h_{12} = \angle h_{22} = 0$.

Scenario V – Symmetric GIC with BPSK: In this example, a symmetric GIC is considered with channel parameters given in Fig. 9. The HK ARR is characterized for BPSK and Gaussian signaling. The obtained ARRs are outerbounded utilizing the results of [17] as shown in the figure. The power allocation is performed for $\Delta R = 0$, $\Delta R = \pm 0.05$, and $\Delta R = \pm 0.15$. For the rate increments during the code optimization, we adopt $\frac{R_{u_i}}{R_{w_i}}, i = 1, 2$, obtained from the power allocation optimization results. Fig. 9 clearly shows that for both symmetric and asymmetric rate pairs the optimized codes are superior to the P2P optimal codes. In addition both P2P and optimized codes beat the naive TS scheme, however, they do not exceed the boundary of the non-naive TS region.

Scenario VI – Symmetric GIC with QPSK: In this example, we consider a symmetric GIC with channel parameters given in Fig. 10. The power allocation optimization is performed for $\Delta R = 0$, $\Delta R = \pm 0.3$, and $\Delta R = \pm 0.4$. It can be observed that, similar to the previous example, the optimized codes beat the P2P codes, both of which outperforming the naive TS rate region. Furthermore, for the asymmetric rate pairs, all the optimized codes and some of P2P codes outperform the non-naive TS rate region.

C. Summary of Results

We now summarize the results obtained in the above examples for GICs with strong and weak interference levels.

This article has been accepted for publication in a future issue of this journal, but has not been fully edited. Content may change prior to final publication. Citation information: DOI 10.1109/TCOMM.2014.2385856, IEEE Transactions on Communications

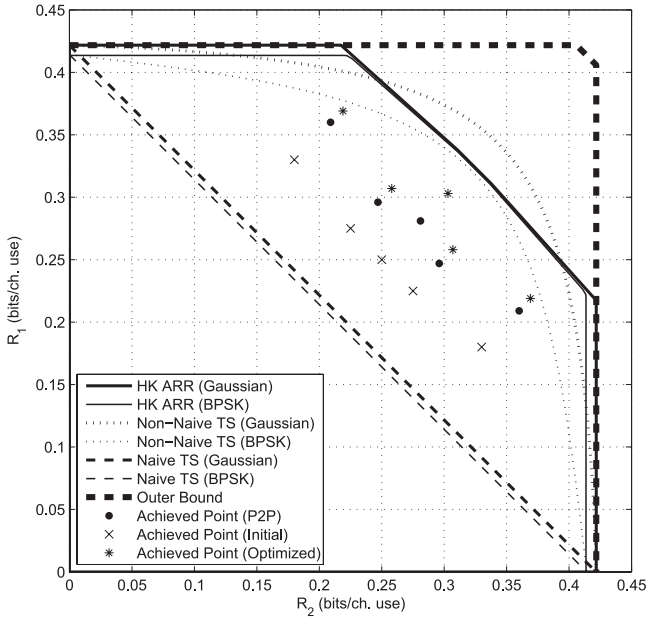

Fig. 9. Scenario V: rate regions and achieved rate pairs for a symmetric GIC with weak interference. $SNR = -4.01$ dB, $INR = -5.01$ dB.

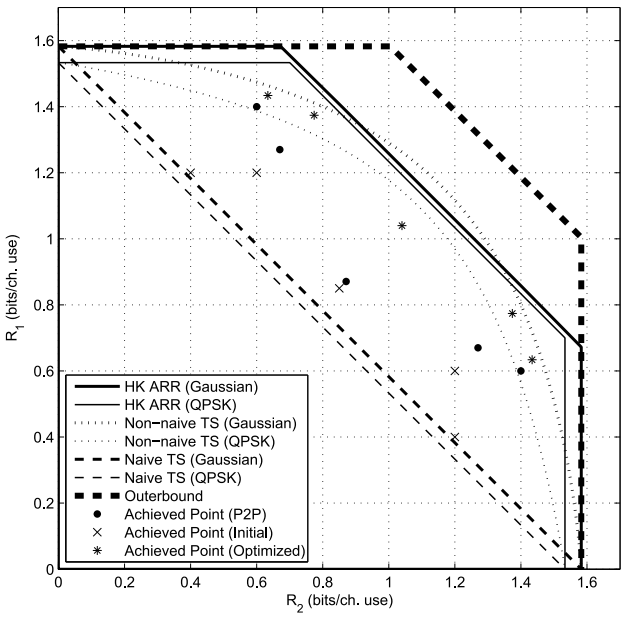

Fig. 10. Scenario VI : rate regions and achieved rate pairs for a GIC with weak interference. $SNR = 3$ dB, $INR = 2.5$ dB, $\angle h_{11} = \angle h_{22} = \frac{\pi}{4}, \angle h_{21} = \angle h_{12} = \frac{\pi}{3}$.

Under strong interference, we see that the optimized codes and the P2P codes outperform both naive TS and non-naive TS schemes. Moreover, the optimized codes consistently improve upon the P2P codes. For all instances with QPSK, the optimized codes also beat non-naive TS scheme for Gaussian signaling, which is not achieved with BPSK. Under weak interference, similar to the case of strong interference, all the optimized codes offer significantly better performance compared to the off-the-shelf P2P codes. In addition, the optimized codes and the P2P codes beat the naive TS schemes for QPSK and Gaussian inputs. Furthermore, the performance of some of the optimized codes is shown to be superior to the non-naive TS results.

We also comment on the results of a recent paper [9] which designs LDPC codes for a symmetric GIC example with weak interference. Considering the method employed, the following distinctions are observed compared with our approach in this paper. First, [9] adopts no superposition at the transmitters, i.e., messages of users are not split into distinct parts. Second, it exploits *soft interference cancellation* wherein the adopted decoder *aims* to decode the interfering signal as well as the desired signal to reduce the effect of interference. Third, it employs density evolution on the factor graphs assuming the *no-interleaver-hypothesis* [3]. This assumption is only valid when identical degree distributions are utilized for both codes, and not applicable to the general case where degree distributions of messages are distinct.

VI. Finite Block Length Code Simulations

A. Random Constructions

In this section, we evaluate the performance of the optimized degree distributions through finite block length code simulations. Parity check matrices are obtained with tools in [28] where most of the length-4 cycles are removed. For the symmetric scenarios, where identical degree distributions are employed at both transmitters, different realizations are utilized in the simulation. The code block lengths are picked as 50k and the maximum number of decoding iterations is set to 500. Fig. 11 shows the decoding results at receiver 1, where for clarity of the presentation we only show the results of the public message or the private message with the worst error rates (i.e., the bottleneck), instead of giving the results for all the messages. Considering a bit error rate (BER) of 10^{-5} as reliable transmission, it can be observed that the decoding results for BPSK and QPSK scenarios are within 0.33 dB and 0.92 dB of the decoding thresholds computed earlier.

B. Algebraic Constructions

We observe that for random constructions the decoding behavior is close to the asymptotic results for large block lengths. However, in practice, LDPC codes with moderate block lengths ($\approx$ 1k) may also be adopted. In this case, a drawback of random designs is the presence of short cycles in the graph which may degrade the decoding performance and may lead to error floors for high SNRs. To remedy this problem, variants of structured LDPC codes have been proposed and studied in the literature [29], [30], where codes are optimized for different parameters, e.g., girth, stopping set, trapping set, minimum distance. Protograph LDPC codes are shown to perform well compared to the other approaches for P2P channels. As the name suggests, the design of these codes is based on a lifted graph from a so-called *base graph*. In [31], protograph LDPC codes are optimized via algebraic designs utilizing *voltage graphs* and *non-abelian groups*, and superior performance is observed compared to the previous designs. In the following, we consider a GIC with strong interference and

This article has been accepted for publication in a future issue of this journal, but has not been fully edited. Content may change prior to final publication. Citation information: DOI 10.1109/TCOMM.2014.2385856, IEEE Transactions on Communications

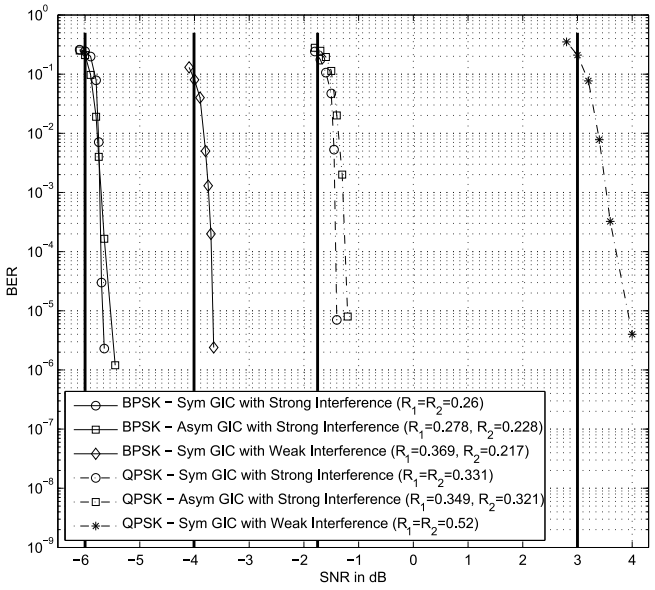

Fig. 11. Finite block length decoding results for specific LDPC codes with random constructions.

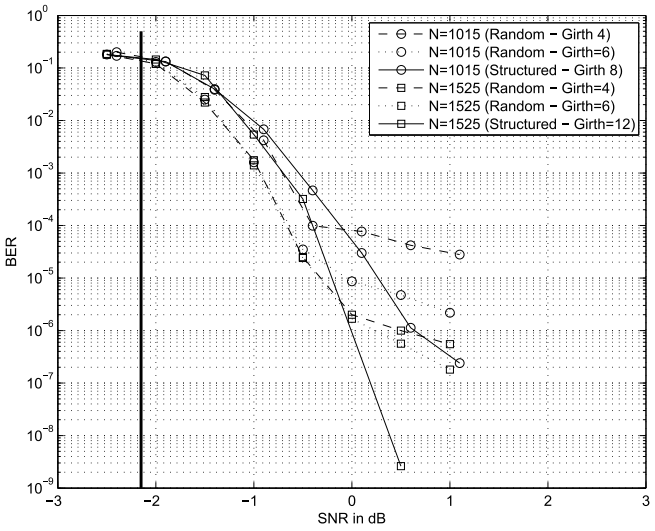

Fig. 12. Decoding results of structured vs. random constructions.

optimize the degree distributions using moderate code block lengths, by employing the systematic approach of [31].

For code optimization, we consider an asymmetric GIC with $SNR_1 = -1$ dB, $INR_1 = -0.25$ dB, $SNR_2 = -1.5$ dB, and $INR_2 = -0.75$ utilizing BPSK with real channel gains. We employ a base matrix with fixed dimensions of 3×5 for both messages. At each iteration, the degree distributions are perturbed by drawing the elements of the base matrix randomly from the set $\{0, 1\}$. Unlike the previous examples, since the dimension of the base matrix does not change throughout the optimization process, we opt for decreasing SNR_i and INR_i at each iteration keeping the signal to interference ratio fixed. The resulting optimized degree distributions $\lambda(x) = 0.3077x + 0.6923x^2$ and $\rho(x) = 0.6154x^3 + 0.3846x^4$ are admissible for the asymmetric GIC with channel parameters $SNR_1 = -2.15$ dB, $INR_1 = -1.4$ dB, $SNR_2 = -2.65$ dB, and $INR_2 = -1.9$. We design the structured codes for block lengths $N = 1015$ and 1525 utilizing non-abelian groups. A non-abelian group of order $m = pq$ is characterized by (p, q, s) where q and p are prime numbers, q divides $p - 1$, and $s^q \equiv 1 \pmod{p}$. The non-abelian groups chosen for $N = 1015$ and $N = 1525$ are (29,7,7) and (61,5,9), respectively. Fig. 12 shows the decoding results for the resulting random and structured constructions. It is observed that for $N = 1015$, error floors occur at 10^{-4} and 4×10^{-5} for random constructions with girths 4 and 6, respectively. On the other hand, an error floor occurs around 10^{-6} for the structured code with girth 8. For $N = 1525$, error floors occur at around 2×10^{-6} for random constructions with girths 4 and 6, however, no error floor is observed for the structured code with girth 12 all the way down to 10^{-9} BER. We also considered the performance of the employed structured codes as a function of the SNRs and INRs at BER 10^{-5} (considered as reliable transmission) and observed that the achieved rate pairs outperform the naive and non-naive TS region for $N = 1015$ and $N = 1525$, respectively.

VII. Conclusions

In this paper, the Han-Kobayashi coding strategy is implemented for two-user Gaussian interference channels. Fixed channel gains are considered and finite constellations are employed for transmission. In order to analyze the behavior of the decoder, a symmetry property is proved for the exchanged LLRs under joint decoding. Moreover, the stability conditions are derived for the degree distributions of the private and public messages under strong and weak interference levels. A code optimization method based on a random perturbation is proposed utilizing a specific instance of differential evolution. Performance of the explicit and implementable LDPC codes (as opposed to information theoretic random codes) are examined through various examples, and promising results are obtained for different scenarios, e.g., strong and weak interference, symmetric and asymmetric rate pairs. Under strong interference, capacity approaching codes are designed which beat even the non-naive TS rate region with Gaussian signaling. Under weak interference, it is observed that the optimized codes operate outside the naive TS rate region (with Gaussian signaling) and for some instances outperform the non-naive TS region. We also note that the designed codes improve consistently upon the codes optimized for P2P channels (used with the same encoding/decoding procedure). Furthermore, simulation results are provided using large block length codes picked from the designed LDPC code ensembles depicting a performance near the predicted limits, and also using random and structured code constructions for small block lengths (on the order of $1k$ bits), demonstrating that the structured codes are superior to the random designs at high SNRs when the block lengths are decreased.

This article has been accepted for publication in a future issue of this journal, but has not been fully edited. Content may change prior to final publication. Citation information: DOI 10.1109/TCOMM.2014.2385856, IEEE Transactions on Communications

APPENDIX
DEGREE DISTRIBUTIONS OF THE OPTIMIZED AND P2P CODES EMPLOYED IN SCENARIOS I-VI

TABLE I
DEGREE DISTRIBUTIONS FOR SCENARIO I.

	Msg.	R	d_c	λ_2	λ_3	λ_4	λ_9	λ_{10}	λ_{19}	λ_{20}	λ_{49}	λ_{50}
P2P	$W_1(W_2)$	0.234	5	0.2790	0.1898	0.1271	0.0679	0.1133	0.0895	0.0093	0.0838	0.0403
Opt.	$W_1(W_2)$	0.26	5	0.2695	0.3292	0.0050	0.1281	0.0246	0.0780	0.0136	0.1428	0.0092
P2P	W_1	0.211	5	0.2845	0.1207	0.1863	0.0539	0.1322	0.0146	0.0091	0.0417	0.1570
	W_2	0.244	5	0.2691	0.2724	0.0219	0.2258	0.0320	0.0432	0.0141	0.0676	0.0539
Opt.	W_1	0.237	5	0.3198	0.0985	0.2097	0.0400	0.0698	0.0037	0.0057	0.0683	0.1845
	W_2	0.274	5	0.2884	0.2563	0.0703	0.0890	0.1329	0.0467	0.0060	0.0394	0.0710
P2P	W_1	0.201	5	0.2717	0.1798	0.1179	0.1454	0.0063	0.0557	0.0273	0.0807	0.1152
	W_2	0.251	5	0.2897	0.1963	0.1024	0.2137	0.0066	0.0388	0.0549	0.0232	0.0744
Opt.	W_1	0.227	5	0.2988	0.1951	0.0890	0.0962	0.0415	0.0420	0.0077	0.1049	0.1248
	W_2	0.277	5	0.2935	0.2555	0.0486	0.1187	0.1137	0.1090	0.0336	0.0124	0.0150
P2P	W_1	0.172	4	0.3494	0.2303	0.1019	0.1463	0.0380	0.0642	0.0043	0.0482	0.0174
	W_2	0.272	5	0.2875	0.2117	0.1342	0.0930	0.0707	0.0610	0.1129	0.0267	0.0023
Opt.	W_1	0.18	4	0.2936	0.3264	0.1352	0.0012	0.1076	0.0332	0.0257	0.0596	0.0175
	W_2	0.28	5	0.2957	0.2261	0.1041	0.0809	0.1319	0.0199	0.0840	0.0393	0.0181
P2P	W_1	0.125	4	0.3321	0.2067	0.1087	0.1679	0.0120	0.0014	0.0059	0.0801	0.0852
	W_2	0.275	5	0.2864	0.2289	0.1014	0.1580	0.0746	0.0155	0.0823	0.0041	0.0488
Opt.	W_1	0.131	4	0.3715	0.1972	0.0594	0.1000	0.0147	0.0320	0.0840	0.0716	0.0696
	W_2	0.281	5	0.3088	0.2130	0.0785	0.1950	0.0657	0.0249	0.0440	0.0296	0.0405

TABLE II
DEGREE DISTRIBUTIONS FOR SCENARIO II.

	Msg.	R	d_c	λ_2	λ_3	λ_4	λ_9	λ_{10}	λ_{19}	λ_{20}	λ_{49}	λ_{50}
P2P	W_1	0.272	5	0.2875	0.2117	0.1342	0.0930	0.0707	0.0610	0.1129	0.0267	0.0023
	W_2	0.172	4	0.3494	0.2303	0.1019	0.1463	0.0380	0.0642	0.0043	0.0482	0.0174
Opt.	W_1	0.282	5	0.3188	0.1587	0.1549	0.0567	0.1369	0.0424	0.0903	0.0274	0.0139
	W_2	0.182	4	0.3708	0.1025	0.2918	0.0147	0.0645	0.0167	0.0445	0.0453	0.0492
P2P	W_1	0.268	5	0.2948	0.2026	0.1153	0.1107	0.0959	0.0188	0.1104	0.0399	0.0116
	W_2	0.218	5	0.2823	0.1020	0.2457	0.0393	0.0500	0.0870	0.0457	0.0234	0.1246
Opt.	W_1	0.278	5	0.3106	0.1901	0.1065	0.1691	0.0809	0.0337	0.0297	0.0033	0.0761
	W_2	0.228	4	0.3815	0.2999	0.0280	0.1453	0.0719	0.0340	0.0074	0.0093	0.0227
P2P	$W_1(W_2)$	0.234	5	0.2790	0.1898	0.1271	0.0679	0.1133	0.0895	0.0093	0.0838	0.0403
Opt.	W_1	0.258	5	0.3007	0.1981	0.1377	0.0228	0.0607	0.0291	0.1192	0.0963	0.0354
	W_2	0.258	5	0.3282	0.1432	0.1499	0.0567	0.0132	0.1182	0.0856	0.0902	0.0148
P2P	W_1	0.202	5	0.2680	0.1786	0.1434	0.0359	0.0667	0.1314	0.0040	0.0141	0.1579
	W_2	0.252	5	0.2799	0.2054	0.1315	0.0421	0.1286	0.1237	0.0078	0.0733	0.0077
Opt.	W_1	0.226	4	0.4126	0.2658	0.0247	0.0933	0.0754	0.0303	0.0176	0.0170	0.0633
	W_2	0.283	5	0.3066	0.2792	0.0384	0.0047	0.0777	0.2256	0.0485	0.0103	0.0090
P2P	W_1	0.186	4	0.3501	0.2414	0.1135	0.0614	0.1191	0.0078	0.0648	0.0089	0.0330
	W_2	0.290	5	0.2954	0.2212	0.1310	0.1526	0.0311	0.0702	0.0592	0.0376	0.0017
Opt.	W_1	0.198	4	0.4218	0.1239	0.1579	0.1236	0.0169	0.0314	0.0191	0.0671	0.0383
	W_2	0.304	5	0.3269	0.1697	0.1583	0.1164	0.1081	0.0261	0.0264	0.0335	0.0346
P2P	W_1	0.134	4	0.3308	0.1876	0.1603	0.1012	0.0377	0.0450	0.0179	0.0292	0.0903
	W_2	0.295	5	0.2816	0.2614	0.1105	0.1229	0.0776	0.0622	0.0598	0.0064	0.0176
Opt.	W_1	0.14	4	0.3283	0.1667	0.2039	0.0596	0.0285	0.0612	0.1450	0.0048	0.0020
	W_2	0.307	5	0.3146	0.2326	0.0770	0.2500	0.0139	0.0701	0.0289	0.0031	0.0098

TABLE III
DEGREE DISTRIBUTIONS FOR SCENARIO III.

	Msg.	R	d_c	λ_2	λ_3	λ_4	λ_9	λ_{10}	λ_{19}	λ_{20}	λ_{49}	λ_{50}
P2P	$W_1(W_2)$	0.302	6	0.2477	0.1277	0.1869	0.1308	0.0093	0.0537	0.0811	0.0633	0.0995
Opt.	$W_1(W_2)$	0.331	6	0.2535	0.2346	0.0814	0.0950	0.0555	0.0287	0.0392	0.0152	0.1969
P2P	W_1	0.245	5	0.2945	0.1266	0.2140	0.0621	0.0478	0.0706	0.0951	0.0497	0.0396
	W_2	0.323	6	0.2467	0.2076	0.0838	0.1042	0.1534	0.0084	0.0480	0.0192	0.1287
Opt.	W_1	0.298	5	0.3413	0.1503	0.2040	0.0167	0.0473	0.0206	0.0376	0.0383	0.1439
	W_2	0.349	6	0.2758	0.1717	0.1256	0.1056	0.1292	0.0116	0.0184	0.0889	0.0732
P2P	W_1	0.23	5	0.2816	0.1623	0.1576	0.1525	0.0045	0.0816	0.0164	0.1408	0.0027
	W_2	0.33	6	0.2148	0.3127	0.0166	0.1485	0.0877	0.0936	0.0077	0.0828	0.0356
Opt.	W_1	0.256	5	0.2134	0.4389	0.0045	0.0357	0.0315	0.0399	0.0179	0.1086	0.1096
	W_2	0.356	6	0.2643	0.2181	0.0876	0.0881	0.1242	0.1050	0.0620	0.0120	0.0387

This article has been accepted for publication in a future issue of this journal, but has not been fully edited. Content may change prior to final publication. Citation information: DOI 10.1109/TCOMM.2014.2385856, IEEE Transactions on Communications

TABLE IV
DEGREE DISTRIBUTIONS FOR SCENARIO IV.

	Msg.	R	d_c	λ_2	λ_3	λ_4	λ_9	λ_{10}	λ_{19}	λ_{20}	λ_{49}	λ_{50}
P2P	W_1	0.345	6	0.2510	0.2298	0.0660	0.2137	0.0370	0.0624	0.0768	0.0076	0.0557
	W_2	0.245	5	0.2945	0.1266	0.2140	0.0621	0.0478	0.0706	0.0951	0.0497	0.0396
Opt. P2P	W_1	0.357	6	0.2605	0.2418	0.0513	0.1876	0.0752	0.0902	0.0107	0.0812	0.0015
	W_2	0.257	5	0.3307	0.1128	0.1725	0.0477	0.0847	0.0977	0.0304	0.0608	0.0627
P2P	W_1	0.33	6	0.2148	0.3127	0.0166	0.1485	0.0877	0.0936	0.0077	0.0828	0.0356
	W_2	0.302	6	0.2477	0.1277	0.1869	0.1308	0.0093	0.0537	0.0811	0.0633	0.0995
Opt. P2P	W_1	0.349	6	0.2607	0.2043	0.1043	0.1252	0.1039	0.0325	0.0685	0.0712	0.0294
	W_2	0.321	6	0.2852	0.1184	0.1285	0.1856	0.0190	0.0723	0.0367	0.0997	0.0546
P2P	W_1	0.263	5	0.2940	0.1676	0.1669	0.1030	0.0940	0.0463	0.0290	0.0679	0.0313
	W_2	0.316	6	0.2345	0.1804	0.1545	0.0309	0.1644	0.0002	0.1018	0.0522	0.0811
Opt. P2P	W_1	0.305	5	0.3028	0.3261	0.0418	0.0147	0.0533	0.0808	0.0787	0.0984	0.0034
	W_2	0.366	6	0.2840	0.2279	0.0762	0.1058	0.0500	0.0616	0.0660	0.0675	0.0610
P2P	W_1	0.24	5	0.2701	0.2186	0.1115	0.0852	0.1123	0.0178	0.0665	0.0638	0.0542
	W_2	0.33	6	0.2148	0.3127	0.0166	0.1485	0.0877	0.0936	0.0077	0.0828	0.0356
Opt. P2P	W_1	0.294	5	0.3339	0.2518	0.0404	0.0393	0.0601	0.0852	0.1227	0.0434	0.0232
	W_2	0.379	6	0.2797	0.3078	0.0062	0.0965	0.0588	0.0649	0.0219	0.0247	0.1395
P2P	W_1	0.219	5	0.2575	0.2490	0.0619	0.1320	0.0768	0.0586	0.0037	0.0494	0.1111
	W_2	0.36	6	0.2511	0.2213	0.1185	0.1178	0.0940	0.0334	0.1323	0.0118	0.0198
Opt. P2P	W_1	0.262	5	0.3020	0.2271	0.1038	0.0633	0.0208	0.0755	0.0317	0.0433	0.1325
	W_2	0.383	6	0.2851	0.1801	0.1842	0.0370	0.1036	0.0256	0.0660	0.0990	0.0194

TABLE V
DEGREE DISTRIBUTIONS FOR SCENARIO V.

	α_1, α_2	Msg.	R	d_c	λ_2	λ_3	λ_4	λ_9	λ_{10}	λ_{19}	λ_{20}	λ_{49}	λ_{50}
P2P	$\alpha_1 = 0.36$	$U_1(U_2)$	0.132	4	0.3315	0.2088	0.1273	0.0790	0.0590	0.0235	0.0508	0.0099	0.1102
	$\alpha_2 = 0.36$	$W_1(W_2)$	0.149	4	0.3613	0.0793	0.2874	0.0251	0.0504	0.0388	0.0596	0.0580	0.0401
Opt.	$\alpha_1 = 0.36$	$U_1(U_2)$	0.142	4	0.3634	0.1674	0.1106	0.0972	0.1013	0.0531	0.0075	0.0628	0.0367
	$\alpha_2 = 0.36$	$W_1(W_2)$	0.161	4	0.3609	0.2671	0.0031	0.0721	0.1386	0.0504	0.0317	0.0325	0.0436
P2P	$\alpha_1 = 0.5$	U_1	0.224	5	0.2659	0.2455	0.0512	0.1661	0.0542	0.0203	0.0415	0.0546	0.1007
	$\alpha_2 = 0$	W_1	0.136	4	0.3488	0.1237	0.2267	0.0161	0.0912	0.0299	0.0422	0.0971	0.0243
		W_2	0.209	5	0.2386	0.2859	0.0504	0.0920	0.0892	0.0326	0.0176	0.1183	0.0754
Opt.	$\alpha_1 = 0.5$	U_1	0.229	5	0.2881	0.1978	0.0867	0.1136	0.0835	0.0679	0.0021	0.0953	0.0650
	$\alpha_2 = 0$	W_1	0.14	4	0.3535	0.2281	0.0474	0.1203	0.0706	0.0037	0.0628	0.0283	0.0853
		W_2	0.217	4	0.3835	0.2263	0.1377	0.0308	0.0711	0.0898	0.0365	0.0097	0.0146
P2P	$\alpha_1 = 0.48$	U_1	0.172	4	0.3494	0.2303	0.1019	0.1463	0.0380	0.0642	0.0043	0.0482	0.0174
	$\alpha_2 = 0.35$	W_1	0.124	4	0.3386	0.1606	0.1633	0.1308	0.0293	0.0175	0.0040	0.1143	0.0416
		U_2	0.112	4	0.3300	0.1874	0.1410	0.0020	0.1268	0.0288	0.0234	0.0481	0.1125
		W_2	0.135	4	0.3400	0.2117	0.1038	0.0594	0.0962	0.0443	0.0348	0.0932	0.0166
Opt.	$\alpha_1 = 0.48$	U_1	0.178	4	0.3814	0.1620	0.1543	0.0896	0.0321	0.0261	0.1088	0.0220	0.0237
	$\alpha_2 = 0.35$	W_1	0.129	4	0.3396	0.2320	0.0639	0.0584	0.1261	0.0294	0.0065	0.0539	0.0902
		U_2	0.117	4	0.3525	0.1999	0.0801	0.0610	0.0203	0.1622	0.0145	0.0085	0.1010
		W_2	0.141	4	0.3359	0.2870	0.0113	0.1037	0.0633	0.0624	0.0216	0.0790	0.0358

TABLE VI
DEGREE DISTRIBUTIONS FOR SCENARIO VI.

	α_1, α_2	Msg.	R	d_c	λ_2	λ_3	λ_4	λ_9	λ_{10}	λ_{19}	λ_{20}	λ_{49}	λ_{50}
P2P	$\alpha_1 = 0.15$	$U_1(U_2)$	0.119	4	0.3270	0.2106	0.1170	0.0227	0.1339	0.0104	0.0259	0.0126	0.1399
	$\alpha_2 = 0.15$	$W_1(W_2)$	0.316	6	0.2345	0.1804	0.1545	0.0309	0.1644	0.0002	0.1018	0.0522	0.0811
Opt.	$\alpha_1 = 0.15$	$U_1(U_2)$	0.143	4	0.3682	0.1303	0.1657	0.0517	0.1055	0.0868	0.0021	0.0358	0.0539
	$\alpha_2 = 0.15$	$W_1(W_2)$	0.377	6	0.3253	0.2005	0.0835	0.0414	0.0536	0.0125	0.0273	0.1647	0.0912
P2P	$\alpha_1 = 0.51$	U_1	0.439	7	0.2110	0.3124	0.0295	0.2368	0.0272	0.1213	0.0336	0.0126	0.0156
	$\alpha_2 = 0$	W_1	0.196	4	0.3650	0.2180	0.1211	0.0224	0.2121	0.0154	0.0020	0.0404	0.0036
		W_2	0.335	6	0.2310	0.2712	0.0518	0.0337	0.2035	0.0197	0.0942	0.0732	0.0217
Opt.	$\alpha_1 = 0.51$	U_1	0.475	7	0.2552	0.2896	0.0379	0.0662	0.2739	0.0364	0.0263	0.0020	0.0125
	$\alpha_2 = 0$	W_1	0.212	4	0.3893	0.2269	0.1236	0.0603	0.0323	0.0486	0.0397	0.0316	0.0477
		W_2	0.387	6	0.3448	0.0318	0.2799	0.0122	0.0958	0.0023	0.1080	0.0455	0.0797
P2P	$\alpha_1 = 0.5$	U_1	0.448	8	0.2019	0.2004	0.1019	0.0789	0.1366	0.1071	0.0559	0.0703	0.0470
	$\alpha_2 = 0$	W_1	0.252	5	0.2799	0.2054	0.1315	0.0421	0.1286	0.1237	0.0078	0.0733	0.0077
		W_2	0.300	6	0.2365	0.2023	0.0902	0.1781	0.0009	0.0784	0.0506	0.1516	0.0114
Opt.	$\alpha_1 = 0.5$	U_1	0.459	7	0.1867	0.3871	0.0485	0.0959	0.1084	0.1263	0.0127	0.0038	0.0306
	$\alpha_2 = 0$	W_1	0.258	5	0.2609	0.3292	0.0059	0.0491	0.1482	0.0740	0.0356	0.0490	0.0481
		W_2	0.317	5	0.3436	0.1022	0.2821	0.0281	0.0774	0.0531	0.0183	0.0113	0.0839

This article has been accepted for publication in a future issue of this journal, but has not been fully edited. Content may change prior to final publication. Citation information: DOI 10.1109/TCOMM.2014.2385856, IEEE Transactions on Communications

REFERENCES

[1] T. Han and K. Kobayashi, "A new achievable rate region for the interference channel," *IEEE Trans. Inf. Theory*, vol. 27, no. 1, pp. 49–60, Jan. 1981.

[2] T. Richardson, M. Shokrollahi, and R. Urbanke, "Design of capacity-approaching irregular low-density parity-check codes," *IEEE Trans. Inf. Theory*, vol. 47, no. 2, pp. 619–637, Feb. 2001.

[3] A. Roumy and D. Declercq, "Characterization and optimization of LDPC codes for the 2-user Gaussian multiple access channel," *EURASIP Journal on Wireless Commun. and Networking*, May 2007, Article ID: 74890.

[4] A. Yedla, P. Nguyen, H. Pfister, and K. Narayanan, "Universal codes for the Gaussian MAC via spatial coupling," in *Proc. Commun., Control, and Computing (Allerton)*, Monticello, Illinois, Sep. 2011, pp. 1801–1808.

[5] P. Berlin and D. Tuninetti, "LDPC codes for fading Gaussian broadcast channels," *IEEE Trans. Inf. Theory*, vol. 51, no. 6, pp. 2173–2182, June 2005.

[6] J. Hu and T. M. Duman, "Low density parity check codes over wireless relay channels," *IEEE Trans. Wireless Commun.*, vol. 6, no. 9, pp. 3384–3394, Sep. 2007.

[7] P. Razaghi and W. Yu, "Bilayer low-density parity-check codes for decode-and-forward in relay channels," *IEEE Trans. Inf. Theory*, vol. 53, no. 10, pp. 3723–3739, Oct. 2007.

[8] M. Khojastepour, N. Ahmed, and B. Aazhang, "Code design for the relay channel and factor graph decoding," in *Proc. 30th Asilomar Conf. on Signals, Syst. and Comput.*, vol. 2, Pacific Grove, California, Nov. 2004, pp. 2000–2004.

[9] A. Bennatan, S. Shamai, and A. Calderbank, "Soft-Decoding-Based Strategies for Relay and Interference Channels: Analysis and Achievable Rates Using LDPC Codes," *IEEE Trans. Inf. Theory*, vol. 60, no. 4, pp. 1977–2009, Apr. 2014.

[10] S. Sharifi, A. K. Tanc, and T. M. Duman, "On LDPC codes for Gaussian interference channels," in *Proc. IEEE Int. Symp. Inf. Theory (ISIT)*, Honolulu, Hawaii, June 2014, pp. 1992–1996.

[11] J. Hou, P. Siegel, L. Milstein, and H. Pfister, "Capacity-approaching bandwidth-efficient coded modulation schemes based on low-density parity-check codes," *IEEE Trans. Inf. Theory*, vol. 49, no. 9, pp. 2141–2155, Sep. 2003.

[12] R. Storn and K. Price, "Differential evolution–A simple and efficient heuristic for global optimization over continuous spaces," *Journal of Global Optimization*, vol. 11, pp. 341–359, Dec. 1997.

[13] A. El Gamal and Y.-H. Kim, *Network Information Theory*. Cambridge University Press, 2011.

[14] H. Chong, M. Motani, and H. Garg, "On the Han–Kobayashi region for the interference channel," *IEEE Trans. Inf. Theory*, vol. 54, no. 7, pp. 3188–3195, July 2008.

[15] H. Sato, "On degraded Gaussian two-user channels," *IEEE Trans. Inf. Theory*, vol. 24, no. 5, pp. 637–640, Sep. 1978.

[16] G. Kramer, "Outer bounds on the capacity of Gaussian interference channels," *IEEE Trans. Inf. Theory*, vol. 50, no. 3, pp. 581–586, Mar. 2004.

[17] R. Etkin, D. Tse, and H. Wang, "Gaussian interference channel capacity to within one bit," *IEEE Trans. Inf. Theory*, vol. 54, no. 12, pp. 5534–5562, Dec. 2008.

[18] A. S. Motahari and A. K. Khandani, "Capacity bounds for the Gaussian interference channel," *IEEE Trans. Inf. Theory*, vol. 55, no. 2, pp. 620–643, Feb. 2009.

[19] T. Richardson and R. Urbanke, *Modern Coding Theory*. Cambridge University Press, 2008.

[20] A. Lampe and J. Huber, "On improved multiuser detection with iterated soft decision interference cancellation," in *Proc. IEEE Commun. Theory Mini-Conf.*, Vancouver, BC, Canada, June 1999, pp. 172–176.

[21] P. Patel and J. Holtzman, "Analysis of a simple successive interference cancellation scheme in a DS/CDMA system," *IEEE J. Sel. Areas Commun.*, vol. 12, no. 5, pp. 796–807, Jun. 1994.

[22] T. Richardson and R. Urbanke, "The capacity of low-density parity-check codes under message-passing decoding," *IEEE Trans. Inf. Theory*, vol. 47, no. 2, pp. 599–618, Feb. 2001.

[23] M. Mondelli, S. H. Hassani, and R. Urbanke, "How to achieve the capacity of asymmetric channels," June 2014, arXiv:1406.7373v2. [Online]. Available: http://arxiv.org/abs/1406.7373

[24] S.-Y. Chung, "On the construction of some capacity-approaching coding schemes," Ph.D. dissertation, Massachusetts Institute of Technology, Cambridge, 2000.

[25] J. Hagenauer, "The EXIT chart–Introduction to extrinsic information transfer in iterative processing," in *Proc. 12th European Signal Process. Conf.*, Vienna, Austria, Sep. 2004, pp. 1541–1548.

[26] S. ten Brink, G. Kramer, and A. Ashikhmin, "Design of low-density parity-check codes for modulation and detection," *IEEE Trans. Commun.*, vol. 52, no. 4, pp. 670–678, Apr. 2004.

[27] M. Franceschini, G. Ferrari, R. Raheli, and A. Curtoni, "Serial concatenation of LDPC codes and differential modulations," *IEEE J. Sel. Areas Commun.*, vol. 23, no. 9, pp. 1758–1768, Sep. 2005.

[28] [Online]. Available: http://itpp.sourceforge.net/4.3.1/

[29] J. Fan, "Array codes as low-density parity-check codes," in *Proc. 2nd Int. Symp. on Turbo Codes and Their Applications*, Sep. 2000, pp. 543–546.

[30] S. Song, L. Lan, S. Lin, and K. Abdel-Ghaffar, "Construction of quasi-cyclic LDPC codes based on the primitive elements of finite fields," in *Proc. Conf. Inf. Syst. and Sci.*, Princeton, New Jersey, Mar. 2006, pp. 835–838.

[31] C. Kelley and J. Kliewer, "Algebraic constructions of graph-based nested codes from protographs," in *Proc. IEEE Int. Symp. Inf. Theory*, Austin, Texas, June 2010, pp. 829–833.

Shahrouz Sharifi (S'10) received the B.S. degree from University of Tehran, Iran, in 2009 and the M.S. degree from Sharif University of Technology, Iran, in 2011. He is currently working towards the PhD degree at Arizona State University. His research interests include various topics in information theory and wireless communications with a particular focus on coding techniques.

A. Korhan Tanc (S'10–M'12) received the Ph.D. degree in Electronics and Communications Engineering from Istanbul Technical University, Turkey, in July 2011. From September 2012 to June 2013, he was a postdoctoral researcher at the School of Electrical, Computer and Energy Engineering, Arizona State University. He is currently an assistant professor at the Department of Electrical and Electronics Engineering, Kirklareli University, Turkey. His research interests include adaptive signal processing, communication theory and multichannel processing.

Tolga M. Duman (S'95–M'98–SM'03–F'11) is a Professor of Electrical and Electronics Engineering Department of Bilkent University in Turkey, and is on leave from the School of ECEE at Arizona State University. He received the B.S. degree from Bilkent University in Turkey in 1993, M.S. and Ph.D. degrees from Northeastern University, Boston, in 1995 and 1998, respectively, all in electrical engineering. Prior to joining Bilkent University in September 2012, he has been with the Electrical Engineering Department of Arizona State University first as an Assistant Professor (1998-2004), then as an Associate Professor (2004-2008), and starting August 2008 as a Professor. Dr. Duman's current research interests are in systems, with particular focus on communication and signal processing, including wireless and mobile communications, coding/modulation, coding for wireless communications, data storage systems and underwater acoustic communications.

Dr. Duman is a Fellow of IEEE, a recipient of the National Science Foundation CAREER Award and IEEE Third Millennium medal. He served as an editor for IEEE Trans. on Wireless Communications (2003-08), IEEE Trans. on Communications (2007-2012) and IEEE Online Journal of Surveys and Tutorials (2002-07). He is currently the coding and communication theory area editor for IEEE Trans. on Communications (2011-present) and an editor for Elsevier Physical Communications Journal (2010-present).